

Article

Production of Saffron Apocarotenoids in *Nicotiana benthamiana* Plants Genome-Edited to Accumulate Zeaxanthin Precursor

Olivia Costantina Demurtas ^{1,*} , Maria Sulli ¹ , Paola Ferrante ¹, Paola Mini ¹, Maricarmen Martí ², Verónica Aragonés ², José-Antonio Daròs ²  and Giovanni Giuliano ^{1,*} 

¹ Biotechnology and Agro-Industry Division, ENEA, Italian National Agency for New Technologies, Energy and Sustainable Economic Development, Casaccia Research Center, 00123 Rome, Italy; maria.sulli@enea.it (M.S.); paola.ferrante@enea.it (P.F.); paola.mini@enea.it (P.M.)

² Instituto de Biología Molecular y Celular de Plantas, Consejo Superior de Investigaciones Científicas-Universitat Politècnica de València, 46022 Valencia, Spain; mamarbo5@alumni.upv.es (M.M.); varagoni@ibmcp.upv.es (V.A.); jadaros@ibmcp.upv.es (J.-A.D.)

* Correspondence: olivia.demurtas@enea.it (O.C.D.); giovanni.giuliano@enea.it (G.G.)

Abstract: Crocins are glycosylated apocarotenoids with strong coloring power and anti-oxidant, anticancer, and neuro-protective properties. We previously dissected the saffron crocin biosynthesis pathway, and demonstrated that the CsCCD2 enzyme, catalyzing the carotenoid cleavage step, shows a strong preference for the xanthophyll zeaxanthin in vitro and in bacterio. In order to investigate substrate specificity in planta and to establish a plant-based bio-factory system for crocin production, we compared wild-type *Nicotiana benthamiana* plants, accumulating various xanthophylls together with α - and β -carotene, with genome-edited lines, in which all the xanthophylls normally accumulated in leaves were replaced by a single xanthophyll, zeaxanthin. These plants were used as chassis for the production in leaves of saffron apocarotenoids (crocins, picrocrocin) using two transient expression methods to overexpress CsCCD2: agroinfiltration and inoculation with a viral vector derived from tobacco etch virus (TEV). The results indicated the superior performance of the zeaxanthin-accumulating line and of the use of the viral vector to express CsCCD2. The results also suggested a relaxed substrate specificity of CsCCD2 in planta, cleaving additional carotenoid substrates.

Keywords: zeaxanthin; *Nicotiana benthamiana*; crocins; picrocrocin; agroinfiltration; agroinoculation; new plant breeding techniques (NPBTs); vacuole



Citation: Demurtas, O.C.; Sulli, M.; Ferrante, P.; Mini, P.; Martí, M.; Aragonés, V.; Daròs, J.-A.; Giuliano, G. Production of Saffron Apocarotenoids in *Nicotiana benthamiana* Plants Genome-Edited to Accumulate Zeaxanthin Precursor. *Metabolites* **2023**, *13*, 729. <https://doi.org/10.3390/metabo13060729>

Academic Editor: Edward Eisenstein

Received: 28 April 2023

Revised: 30 May 2023

Accepted: 3 June 2023

Published: 6 June 2023



Copyright: © 2023 by the authors. Licensee MDPI, Basel, Switzerland. This article is an open access article distributed under the terms and conditions of the Creative Commons Attribution (CC BY) license (<https://creativecommons.org/licenses/by/4.0/>).

1. Introduction

Crocins are high-value hydrophilic pigments that accumulate at high concentrations in the stigmas and/or tepals of different *Crocus* (Iridaceae) flowers and reach particularly high levels in the stigmas of *Crocus sativus* (saffron), the most expensive spice in the world [1,2]. We and others have previously dissected the biosynthetic pathway in *Crocus* stigmas (Figure 1). The first dedicated step is the 7,8/7',8' cleavage of zeaxanthin by carotenoid cleavage dioxygenase 2 (CsCCD2) [3], followed by dehydrogenation of crocetin dialdehyde by CsALDH3I1 and primary glycosylation by CsUGT74AD1 [4]. Secondary glycosylation is exerted by CsUGT91P3 [5]. The cleavage of zeaxanthin at the 7,8/7',8' double bonds also produces OH- β -cyclocitral [3] that is glycosylated to picrocrocin, by the activity of CsUGT709G1 [6]. Picrocrocin and the derived volatile apocarotenoid, named safranal, are responsible for the characteristic saffron taste and aroma, respectively.

The crocin pathway is highly compartmentalized (Figure 1): CsCCD2 is localized into the plastid, CsALDH3I1 in the endoplasmic reticulum, and CsUGT74AD1 in cytoskeleton-like cytoplasmic structures [4]. Crocins are transported into vacuoles by ABCC-type transporters [7].

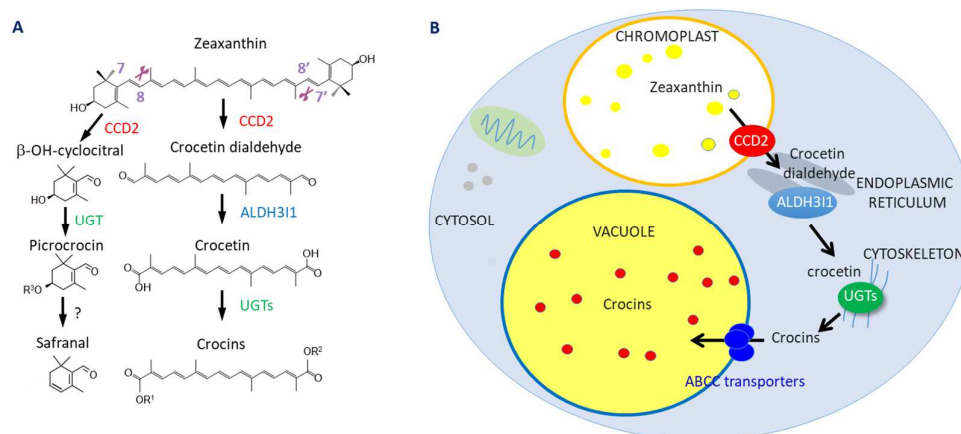


Figure 1. (A) Crocin-picrocrocins-safranal biosynthesis pathway in *C. sativus*, and (B) its subcellular compartmentation. R¹ and R² in panel A are sugars or H atoms, as previously described [4], R³ is a glucose, as previously described [6].

The crocin biosynthesis pathway has also been elucidated in *Gardenia jasminoides* [8] and partially in *Buddleja davidii* [9,10] and *Bixa orellana* [11]. In these cases, a CCD4 is involved in the carotenoid cleavage step.

Different crocin-synthesizing CCDs show different substrate specificities in bacterio and/or in vitro: the *Crocus* and *Buddleja* CCDs cleave preferentially zeaxanthin [3,9], while the *Gardenia* and *Bixa* enzymes have a more relaxed substrate specificity, cleaving lycopene, beta-carotene, and zeaxanthin [8,11].

Interestingly, expression in planta of the above CCDs is sufficient for crocin accumulation, suggesting that the ALDH and UGT activities are endogenously expressed in plant tissues. Heterologous expression systems include maize endosperm [3], rice and citrus calli [12,13], *Nicotiana benthamiana* leaves [7,11,14], transplastomic tobacco leaves [11], *N. tabacum* and *N. glauca* leaves [15,16], and transgenic tomato fruits [11,17]. Since many of these tissues contain a variety of different carotenoids, but very low to null levels of zeaxanthin, the question arises about which are the in planta carotenoid substrates of CCDs with narrow substrate specificity, such as CsCCD2. This question is particularly relevant to develop a bio-factory system to produce the valuable crocins in heterologous plants. To answer this question, we generated genome-edited plants of *N. benthamiana* in which the normal leaf xanthophyll complement (lutein, violaxanthin, antheraxanthin, and neoxanthin) was replaced by zeaxanthin, a xanthophyll that is normally accumulated in leaves only under high-light conditions (Sulli et al., unpublished). In this report we used both *Agrobacterium tumefaciens*-mediated infiltration, and inoculation with a custom-built tobacco etch virus (TEV; genus *Potyvirus*; family *Potyviridae*), to overexpress the saffron CsCCD2 dioxygenase, which catalyzes the first dedicated step in crocin biosynthesis. Results suggested that depending on the overexpression method used, CsCCD2 showed relaxed substrate specificity in planta, also cleaving lutein and, to a lesser extent, violaxanthin and β -carotene. Remarkably, we obtained a maximum apocarotenoid and crocin yields (1129.6 and 883.7 $\mu\text{g g}^{-1}$ dry weight (DW), respectively) in genome-edited plants with the highest levels of zeaxanthin, in which CsCCD2 was expressed with the viral vector.

2. Materials and Methods

2.1. Plant Material

N. benthamiana laboratory isolate (LAB) plants [18], edited in the two homologous *Lycopene ϵ -cyclase* (LCYe) and two *Zeaxanthin epoxidase* (ZEP) genes (LCYe1-LCYe2: *Nbv6.1trP33255-Nbv6.1trP19906*; ZEP1-ZEP2: *Nbv6.1trP61527-Nbv6.1trP32819*) [19] (Sulli et al., unpublished) were utilized. Two different high zeaxanthin (HZ) lines were utilized: HZ-9

(*lcy1lcy2ZEP1zep2*) in which only one of the two *ZEP* genes was inactivated, and HZ-11 (*lcy1lcy2zep1zep2*) in which both *ZEP* genes were inactivated.

2.2. Agroinfiltration

Wild-type (Wt) and HZ plants were grown in soil for 5–6 weeks in a growth chamber with controlled temperature (22 °C) and photoperiod (16 h light/8 h dark, 150 $\mu\text{E m}^{-2} \text{s}^{-1}$, given from five Lumilux Cool Daylight L 58W/865 and one Fluora L 58W/77 fluorescent lamps, Osram, Germany). Agroinfiltration was performed by inoculating sub-apical leaves of the second and third whorls, as previously described [7,11]. For each plant, the 4 sub-apical leaves of each agroinfiltrated plant were harvested at 5 days post inoculation (dpi), pooled, and frozen in liquid nitrogen. Three independent experiments were performed. *N. benthamiana* Wt and HZ lines were co-infiltrated with *A. tumefaciens* C58C1 cells containing pBI121:CsCCD2 [7] or pBI121 [20] as negative control, and the RK19 silencing suppressor [21].

2.3. Virus Inoculation

Plasmid pGTEV:CsCCD2 was built using standard molecular biology techniques with the corresponding restriction enzymes (Thermo Fisher Scientific, Waltham, MA, US) and T4 DNA ligase (Thermo Fisher Scientific, Waltham, MA, US). The Eco81I-ApaI DNA fragment of pGTEV Δ NiB-CsCCD2L [14] was replaced by the same restriction fragment from pGTEVa [22]. This plasmid contains a full-length TEV infectious clone including the viral NiB cistron. pGTEV-eGFP is a pGTEVa derivative that contains the cDNA of the enhanced GFP (AAB08060) inserted between the viral NiB and CP cistrons [23]. The GFP cDNA is flanked by sequences corresponding to artificial NiAPro cleavage sites that mediate the release of the recombinant protein from the viral polyprotein [23]. The full nucleotide sequences of recombinant viruses TEV-CsCCD2L and TEV-eGFP are shown in Figure S1. Empty plasmid pG35Z was used to mock-inoculate plants [24]. *A. tumefaciens* C58C1, harboring the helper plasmid pCLEAN-S48 [25], were transformed with plasmids pGTEV:CsCCD2L, pGTEV:GFP, and pG53Z, and selected in plates containing 50 $\mu\text{g mL}^{-1}$ rifampicin, 50 $\mu\text{g mL}^{-1}$ kanamycin, and 7.5 $\mu\text{g mL}^{-1}$ tetracycline. Selected colonies were grown overnight at 28 °C in Luria-Bertani (LB) liquid media containing 50 $\mu\text{g mL}^{-1}$ kanamycin. Cells were brought to optical density (600 nm) of 0.5 in 10 mM MES-NaOH, pH 5.6, 10 mM MgCl_2 , and 150 μM acetosyringone, and *Vir* genes induced for 2 h at 28 °C. Using a needleless syringe, cultures were infiltrated in the abaxial side of two leaves of five-week-old *N. benthamiana* Wt and genome-edited (HZ-9 and HZ-11) plants. After agroinoculation, plants were cultured in a growth chamber at 25 °C under a 12 h day–night photoperiod with an average photon flux density of 240 $\mu\text{E m}^{-2} \text{s}^{-1}$. Symptomatic systemic leaves were collected at 10 dpi and processed for metabolite analysis.

2.4. Extraction and Analysis of Carotenoids

Carotenoids were extracted from 10 mg of ground, lyophilized leaf tissue under dim laboratory light conditions ($<5 \mu\text{E m}^{-2} \text{s}^{-1}$) during the entire extraction procedure. Samples were homogenized (20 min, 30 Hz) with 1.8 mL 100% cold acetone spiked with 50 mg L^{-1} of internal standard (DL- α -tocopherol acetate, Sigma-Aldrich, Cat. No. 47786, St. Louis, MO, USA), using the TissueLyser MM300 (Retsch, Haan, Germany). Samples were centrifuged (15 min, 20,000 $\times g$, 4 °C), and supernatant was transferred in two new tubes. A quantity of 0.8 mL acetone was directly transferred into a new tube, centrifuged (15 min, 20,000 $\times g$, 4 °C), and 0.6 mL of the supernatant was filtered using WhatmanTM Mini-UniPrepTM Amber Syringeless Filter vials (0.45 μm PTFE, Merck, Darmstadt, Germany) for LC analysis. A quantity of 0.9 mL was directed to saponification, and thus transferred to a 2 mL tube containing 100 mg of Ambersep 900 OH resin (Merck, Darmstadt, Germany), which was pre-treated with ultrapure water (LiChrosolv[®], Merck, Darmstadt, Germany) as previously described [26]. After shaking for 1 h in the dark and centrifugation (15 min, 14,000 $\times g$, 4 °C), 0.6 mL of supernatant was removed and transferred into filtered WhatmanTM Mini-

UniPrep™ Amber Syringeless Filter vials (0.45 µm PTFE, Merck, Darmstadt, Germany) for LC analysis. Based on previous experience, this protocol results in recovery efficiencies >90%. Analytical HPLC was carried out on a LC-PhotoDiode Array (PDA) system (Accela, Thermo Fisher Scientific, Waltham, MA, USA). LC separation was performed using a Carotenoid C30 column (100 × 3 mm², 3-µm particle size) (YMC, Dinslaken, Germany) and the column temperature was 25 °C. The elution system was A, MeOH; B, MeOH/water (4:1 *v/v*) with 0.2% ammonium acetate; and C, tert-Butyl methyl ether (C). The gradient was 0 to 1.2 min 95% A, 5% B; 3.5 min 80% A, 5% B; 6.8 min 30% A, 5% B, 65% C; 16 min 95%, 5% B. PDA data were recorded in the 200–700 nm range [27]. Chromatographic flux after equilibration was 0.8 mL/min and total run time was 18 min, and the injection volume was 10 µL. All the solvents used were LC grade (Merck, Darmstadt, Germany). For quantification, carotenoid peaks were integrated at their individual λ_{\max} and DL- α -tocopherol acetate at 285 nm as previously described [28]. Data were then normalized on the peak area of the internal standard and on the dry weight of leaf tissue used for the extraction [29–32]. The limits of detection and quantitation for individual carotenoid peaks were 1500 and 2000 µAU, respectively.

2.5. Extraction and Analysis of Crocins

Semi-polar metabolites were extracted as previously described with some modifications [11]. Briefly, 10 mg of powder was ground and resuspended in 750 µL of 75% (*v/v*) cold methanol spiked with 0.5 µg mL⁻¹ formononetin (Sigma-Aldrich, Cat. No. 47752-25MG-F, St. Louis, MO, USA) with vigorous agitation for 30 min at 25 °C. Samples were then centrifuged at 20,000 × *g* for 20 min; the supernatant was collected, filtered with HPLC PTFE filter tubes (0.22 µm pore size), and subjected to high performance liquid chromatography-photodiode array detection-high resolution mass spectrometry (LC-PDA-HRMS) analysis using a Q-Exactive mass spectrometer (Thermo Fisher Scientific, Waltham, MA, USA) as previously described [4]. Based on previous experience, this protocol results in recovery efficiencies >90%. Briefly, the separation was performed by injecting 5 µL of sample on a C18 Luna reverse-phase column (100 × 2.1 mm², 2.5 µm; Phenomenex, Torrance, CA, USA) using as mobile phases water + 0.1% formic acid (A) and acetonitrile + 0.1% formic acid (B) at a total flow rate of 250 µL/min. The separation was developed using 5% B for 0.5 min, followed by a 24 min linear gradient to 75% B. The ionization of polar and semi-polar apocarotenoids was performed using a heated electrospray ionization (HESI, Thermo Fisher Scientific, Waltham, MA, USA) source with nitrogen used as a sheath and auxiliary gas, set to 45 and 30 units, respectively. The vaporizer temperature was 270 °C, the capillary temperature was 30 °C, the discharge current was set to 5 µA, and the S-lens RF level was set at 50. The acquisition was performed in the mass range 110–1600 *m/z* both in positive and in negative ion modes with the following parameters: resolution 70,000, microscan 1, AGC target 1 × 10⁶, maximum injection time 50. All the solvents used were LC-MS grade (Merck, Darmstadt, Germany). PDA data were recorded in the 200–700 nm range. Crocins, crocetin, picrocrocins, and OH- β -cyclocitral were identified in positive ionization mode in LC-MS and LC-MS/MS chromatograms and quantified in PDA chromatograms as follows: crocin and crocetin peak areas were integrated at their λ_{\max} = 443 nm, picrocrocins and OH- β -cyclocitral at λ_{\max} = 257 nm, and the internal standard formononetin at λ_{\max} = 256 nm; the areas were quantified considering the specific extinction coefficients ($\epsilon_{1\%}$) of each compound, using the $\epsilon_{1\%}$ values reported for crocins and crocetins [33], for picrocrocins and its precursor OH- β -cyclocitral [34], and for the internal standard (formononetin) [35]. Data were then normalized on the peak area of the internal standard and on the dry weight of leaf tissue used for the extraction. The limits of detection and quantitation for individual crocin/picrocrocins peaks were 1000 and 1500 µAU, respectively.

2.6. Statistical Analyses

The Past software (version 3.11) [36] was used to identify carotenoids/apocarotenoids showing statistically significant differences between different experimental points.

2.7. Confocal Microscopy

Laser scanning confocal microscopy (LSCM) analysis of *N. benthamiana* tissues from inoculated plants was performed using a Zeiss 7080 Axio Observer (Zeiss, Oberkochen, Germany) equipped with a C-Apochromat 40X/1.20 W corrective water immersion objective lens. For the multicolor detection of crocins and chlorophylls, imaging was performed using the sequential channel acquisition mode. A 458 nm laser was used for excitation of crocin and chlorophyll autofluorescence, which was detected from 465 to 620 nm and from 690 to 740 nm, respectively. Images were processed using the FIJI software (Dresden, Germany), "<http://fiji.sc/Fiji>" (accessed on 4 April 2021).

3. Results and Discussion

3.1. Selection of Edited Lines as Chassis for the Production of Crocins

The LAB strain of *N. benthamiana* [18] and two previously constructed, high zeaxanthin (HZ) genome-edited lines, in the same genetic background, were utilized. Briefly, two homologous *Lycopene ϵ -cyclase* (*LCYe1* and *LCYe2*) and two *Zeaxanthin epoxidase* (*ZEP1* and *ZEP2*) genes present in the *N. benthamiana* allotetraploid genome were targeted. Two different edited lines were obtained: HZ-9 (*lcy1lcy2ZEP1zep2*) in which only one of the two *ZEP* genes was inactivated, and HZ-11 (*lcy1lcy2zep1zep2*) in which both *ZEP* genes were inactivated (Sulli et al., unpublished). In both lines, ϵ -branch (lutein) and β -branch (violaxanthin and neoxanthin) xanthophylls were completely replaced by zeaxanthin, which is undetectable in Wt lines (Figure 2A). Zeaxanthin levels were higher in the HZ-11 line, which exhibits a more stunted phenotype, probably due to a more severe deficiency in abscisic acid biosynthesis (Figure S2). These lines were used as chassis for crocin production, through the overexpression of *CsCCD2* using two transient approaches: agroinfiltration using the pBI:121 vector [20] and virus-based expression using TEV [14] (Figure 2B). The latter, based on a viral vector able to replicate and move systemically through the plant, was expected to achieve larger *CsCCD2* accumulation [14,37].

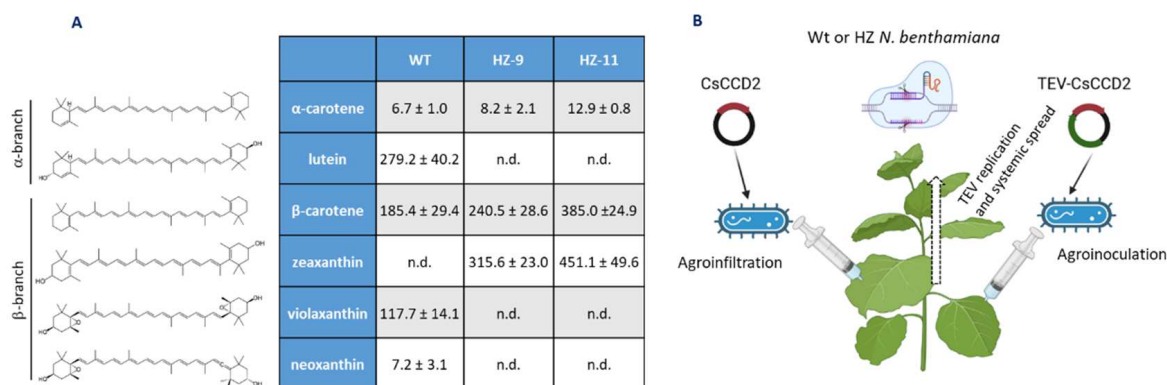


Figure 2. Production of saffron crocins in genome-edited *N. benthamiana*. **(A)** Carotenoid composition ($\mu\text{g g}^{-1}$ dry weight (DW); average values \pm standard deviation of three biological replicates) of Wt, HZ-9 (*lcy1lcy2ZEP1zep2*) and HZ-11 (*lcy1lcy2zep1zep2*) *N. benthamiana* lines (nd = not detectable); carotenoid structures are shown on the left. **(B)** Approaches used to overexpress *CsCCD2* in Wt or HZ *N. benthamiana* plants.

3.2. Agroinfiltration

Leaves of Wt and HZ lines were co-infiltrated with *A. tumefaciens* harboring either pBI121 or pBI121:*CsCCD2*, and with another strain harboring the RK19 silencing suppressor [7]. Upon visual inspection, agroinfiltration of HZ-9 leaves was comparable to that

of Wt leaves, while HZ-11 leaves proved much more difficult to agroinfiltrate, possibly due to a thickening of the leaf cuticle as a consequence of altered ABA levels (Sulli et al., unpublished). At 5 dpi, several novel apocarotenoids, attributable to the action of CCD2, accumulated in Wt leaves agroinfiltrated with CsCCD2: OH- β -cyclocitral, picrococin, crocetins, and crocins. Total apocarotenoids accumulated to $38.4 \mu\text{g g}^{-1}$ DW and crocins to $20.3 \mu\text{g g}^{-1}$ DW (Figure 3A, Table S1).

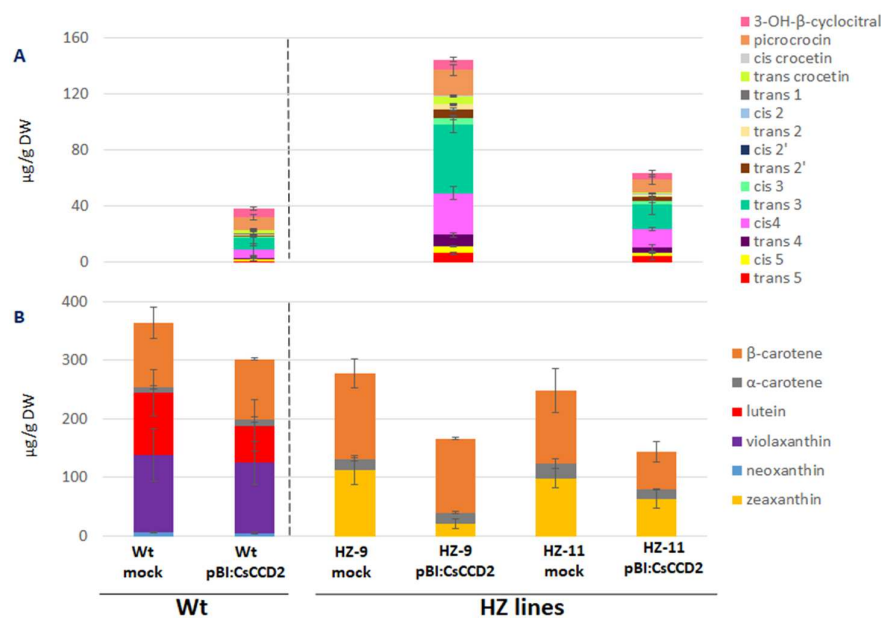


Figure 3. Apocarotenoid (A) and carotenoid (B) levels in Wt and HZ *N. benthamiana* plants, agroinfiltrated with pBI121 (mock) and pBI121:CsCCD2. Average values with standard deviations of three independent experiments are presented. Quantitative data can be found in Tables S1 and S2.

A strong increase in total apocarotenoid and crocin levels (147.2 and $115.3 \mu\text{g g}^{-1}$ DW, respectively) was observed in HZ-9 leaves, which contain higher levels of zeaxanthin, the CsCCD2 preferred substrate. In HZ-11 leaves, in spite of the higher levels of zeaxanthin, much lower total apocarotenoid and crocin levels were observed (63.4 and $48.9 \mu\text{g g}^{-1}$ DW, respectively), probably due to the less efficient agroinfiltration process. The relative abundance of different crocin isomers in leaves of Wt, HZ-9, and HZ-11 plants was similar, with *trans*-crocin 3 being the most abundant isomer, followed by *cis*-crocin 4. In addition, in the HZ lines we observed an increase in the accumulation of hyperglucosylated crocins, *trans* and *cis*-crocin 5, compared to the Wt.

The levels of zeaxanthin in HZ-9 and HZ-11 leaves were reduced upon CsCCD2 overexpression (Figure 3B, Table S2). β -carotene levels were somewhat reduced in HZ-11, but not HZ-9 leaves. In Wt leaves, which contain undetectable levels of zeaxanthin, lutein was the major carotenoid showing significant reduction upon CsCCD2 overexpression. These results are compatible with the fact that zeaxanthin and lutein differ only by the position of a double bond in one of the two ionone rings and with our previous results [3], showing that both zeaxanthin and lutein were substrates for CsCCD2 in vitro, yielding respectively 3-OH- β -apo-8'-carotenal and 3-OH- ϵ -apo-8'-carotenal, both of which are possible crocetin dialdehyde precursors.

3.3. Viral Expression

We also investigated CsCCD2 overexpression using a TEV vector [14] as a second means to overexpress CsCCD2 in leaves of Wt and HZ *N. benthamiana* lines. Previous experiments expressing CsCCD2 in *N. benthamiana* plants used a TEV vector with a deletion in the viral nuclear inclusion b (NIb) cistron (TEV Δ NIb) to increase cargo capacity [14]. Therefore, the resulting viral recombinant clone only replicated and moved in plants in

which the Nib was supplied in *trans*, such as in a transformed *N. benthamiana* line in which this viral protein was expressed under the control of cauliflower mosaic virus 35S promoter and terminator [14]. To circumvent this requirement, in this work we built a new recombinant clone based on full-length TEV, able to replicate and move in *N. benthamiana* genotypes not carrying the 35S:Nib transgene. In this vector, CsCCD2 is expressed as the first gene product of the viral polyprotein, since this position in the viral polyprotein is crucial to efficiently target the chloroplast [23] (Figure 4). Two additional vectors, carrying the GFP (Figure 4), and an empty vector, were used as controls. The three vectors are respectively named TEV:CsCCD2, TEV:GFP, and TEV for simplicity.

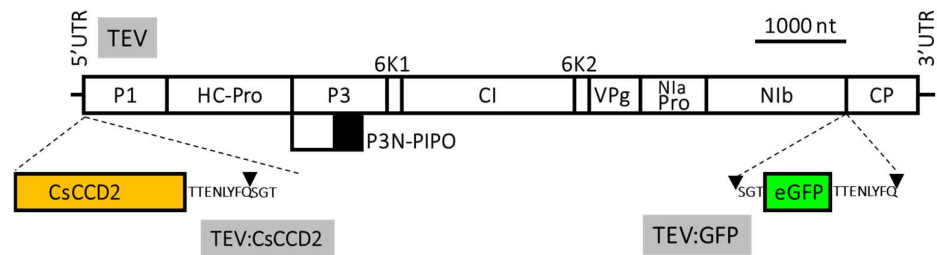


Figure 4. Schematic representation of wild-type TEV and recombinant clones TEV:CsCCD2 and TEV:GFP. CsCCD2 and eGFP cDNAs are represented by orange and green boxes, respectively. Lines represent TEV 5' and 3' UTR and boxes represent P1, HC-Pro, P3, P3N-PIPO, 6K1, CI, 6K2, VPg, NIaPro, Nib, and CP cistrons, as indicated. The sequences of the artificial NIaPro cleavage sites to mediate the release of the recombinant proteins from the viral polyprotein are also indicated. The black triangle indicates the exact cleavage site. Scale bar corresponds to 1000 nt.

Inoculation of Wt plants with TEV:CsCCD2 yielded much higher apocarotenoid and crocin levels (660.1 and $483.1 \mu\text{g g}^{-1}$ DW, respectively) compared to agroinfiltration (Figure 5A, Table S3). These levels were further boosted in leaves of the HZ-9 and HZ-11 lines, with the latter showing the highest levels (1129.7 and $883.7 \mu\text{g g}^{-1}$ DW, respectively). Also in this case, picrocrocin and OH- β -cyclocitral accumulated at higher levels both HZ-9 lines compared to the Wt, and comparable levels were detected between the two edited lines (Figure 5A, Table S3).

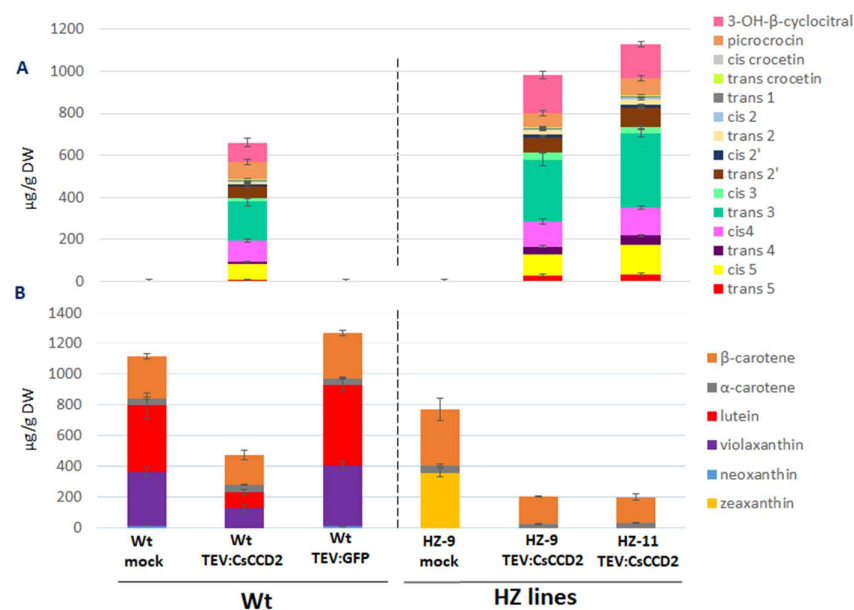


Figure 5. Apocarotenoid (A) and carotenoid (B) levels in Wt and HZ *N. benthamiana* plants, inoculated with TEV, TEV:GFP, and TEV:CsCCD2. Average values with standard deviations of three independent experiments are presented. Quantitative data are shown in Tables S3 and S4.

Zeaxanthin was reduced to undetectable levels in both lines, while β -carotene showed a 51–53% reduction upon TEV:CsCCD2 inoculation, depending on the inoculated line (Figure 5B, Table S4). This indicates that zeaxanthin is the preferred in planta substrate for CsCCD2 and that, contrary to agroinfiltration, virus-based expression functions equally well on HZ-9 and HZ-11 lines, likely because self-replication and systemic spread of the virus overcomes the mechanical or physiological obstacles preventing efficient agroinfiltration of the latter line.

In Wt plants, where zeaxanthin is undetectable, a strong reduction in lutein, neoxanthin, and violaxanthin was observed upon TEV:CsCCD2 inoculation, suggesting that, in the absence of zeaxanthin, the latter xanthophylls become CsCCD2 substrates. Again, β -carotene showed lower (29%) reduction with respect to xanthophylls (Figure 5B, Table S4).

Taken together, these data suggest the following scenario: (i) zeaxanthin is the preferred substrate for CsCCD2 cleavage in *N. benthamiana* leaves, followed by lutein, neoxanthin, violaxanthin, and β -carotene; (ii) the higher expression levels obtained via TEV relax the observed substrate specificity of CsCCD2, making it able to cleave neoxanthin and violaxanthin, two xanthophylls that are not cleaved upon agroinfiltration; (iii) the highest crocin levels are reached in HZ-11 plants, indicating that genome editing and a virus-based expression system play additive roles in achieving maximal crocin production.

The different amenabilities of the different carotenoids to cleavage by CsCCD2 in leaves are probably due to their different structures (Figure 2), but their different localizations in the photosynthetic protein-pigment complexes could also play a role: while xanthophylls such as lutein, violaxanthin, zeaxanthin, and neoxanthin are localized in the peripheral light-harvesting complexes, β -carotene is localized exclusively in photosystem II, and preferentially in photosystem I reaction centers, where it could be less accessible to CsCCD2 cleavage [38,39].

3.4. Endogenous Factors and Their Contribution to Crocin Accumulation

HZ leaves, in which CsCCD2 is expressed either by simple agroinfiltration or using a viral vector, not only show quantitative differences in crocin accumulation, but also qualitative differences in the types of apocarotenoids accumulated (Figure 6, Tables S1 and S3). Agroinfiltrated leaves show a higher fraction of highly glycosylated crocins (48% crocins 4 and 5) than those that were virus-inoculated (40%). This is an indirect indication that the higher apocarotenoid levels achieved by the viral vector may saturate the endogenous ALDH and UGT activities present in *N. benthamiana* leaves.

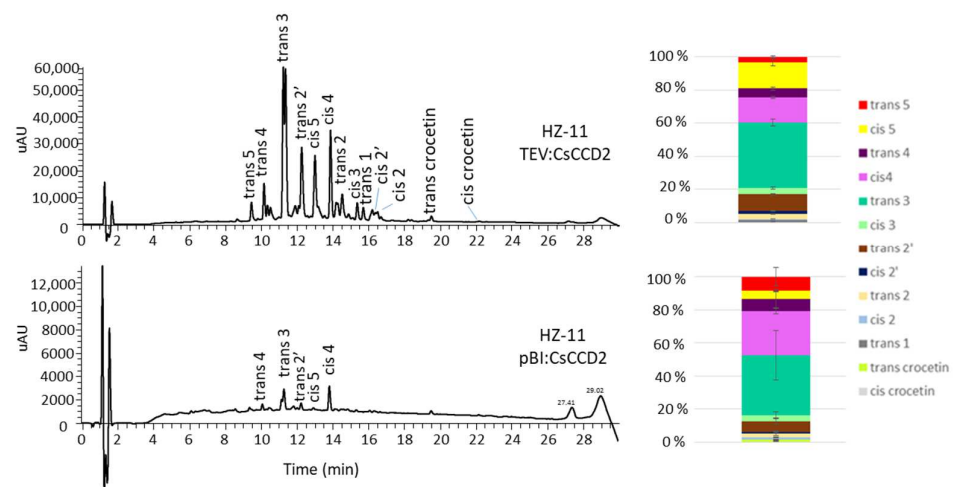


Figure 6. Crocin accumulation in leaves of the HZ-11 line expressing the CsCCD2 enzyme by a viral vector (TEV:CsCCD2) or agroinfiltration (pBI:CsCCD2). Quantitative data are shown in Tables S1 and S3.

Another factor contributing to accumulation of crocins is their sequestration into vacuoles [7,40]. Co-agroinfiltration of the CsABCC4a transporter in *N. benthamiana* leaves together with CsCCD2 increases the levels of crocins, indicating that endogenous vacuolar transport in *N. benthamiana* leaves may be rate-limiting for crocin accumulation [7]. Qualitative evaluation of vacuole-localized crocin autofluorescence in Wt, HZ-9, and HZ-11 leaves infected with TEV:CsCCD2 by LSCM indicates that vacuole-localized crocin fluorescence is stronger in HZ than in Wt leaves (Figure 7). We hypothesize that, as demonstrated in the case of other vacuolar transporters [41], the endogenous *N. benthamiana* transporters mediating vacuolar localization of crocins are induced by the increased abundance of their substrate. This hypothesis could be tested by transcriptomic analyses of TEV:CsCCD2-infected plants in comparison with an empty vector control.

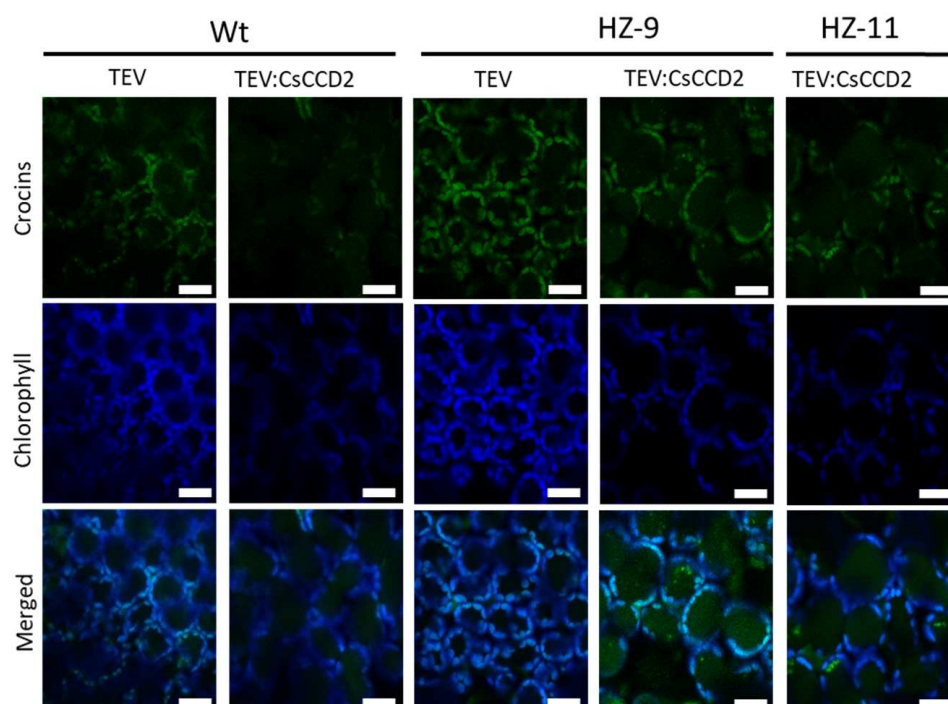


Figure 7. LSCM images of crocins (green) and chlorophyll autofluorescence (blue) from symptomatic Wt and HZ leaves, infected with TEV or TEV:CsCCD2, at 12 dpi. Scale bars indicate 20 μm .

4. Conclusions

N. benthamiana is a promising bio-factory system for the production of biopharmaceuticals and small molecules, and new plant-breeding techniques such as genome editing, agroinfiltration, and the use of viral vectors are powerful tools to deploy its full potential [42]. In this work, we demonstrated that a combination of methodologies can be used to further boost the production of saffron apocarotenoids, mainly crocins, in *N. benthamiana* leaves, as well as to study the in planta substrate specificities of carotenoid cleavage enzymes.

Supplementary Materials: The following supporting information can be downloaded at: <https://www.mdpi.com/article/10.3390/metabo13060729/s1>, Figure S1: Nucleotide sequences of wild-type TEV (sequence variant DQ986288 with two silent mutations G273A and A1119G, in red) and the derived recombinant viruses TEV-CsCCD2L and TEV-eGFP; Figure S2: Representative wt and HZ edited plants used in this study, 8 weeks after seed sowing; Table S1: Apocarotenoid accumulation ($\mu\text{g g}^{-1}$ DW) in different mock and pBI:CsCCD2 agroinfiltrated lines; Table S2: Carotenoid composition ($\mu\text{g g}^{-1}$ DW) of different mock and agroinfiltrated lines; Table S3: Apocarotenoid accumulation ($\mu\text{g g}^{-1}$ DW) in different mock and TEV-inoculated lines; Table S4: Carotenoid composition ($\mu\text{g g}^{-1}$ DW) of different mock and TEV-inoculated lines.

Author Contributions: Conceptualization, O.C.D., G.G. and J.-A.D.; data curation, O.C.D., M.S., P.F., M.M. and V.A.; formal analysis, O.C.D. and M.S.; investigation, O.C.D., M.S., P.F., P.M. and M.M.; methodology, O.C.D. and M.S.; project administration, O.C.D. and G.G.; validation, O.C.D., M.S., M.M. and V.A.; visualization, O.C.D., M.S., M.M., V.A., J.-A.D. and G.G.; writing—original draft, O.C.D., M.S., J.-A.D. and G.G.; writing—review and editing, O.C.D., M.S., J.-A.D. and G.G.; resource, P.F. and P.M.; supervision, G.G.; funding acquisition, J.-A.D. and G.G. All authors have read and agreed to the published version of the manuscript.

Funding: Work supported by the European Commission, Horizon 2020 program (Project NEW-COTIANA, grant agreement 760331), and the Spanish Ministerio de Ciencia e Innovación through Agencia Estatal de Investigación (PID2020-114691RB-I00). MM was the recipient of a predoctoral contract (FPU16/05294) from the Ministerio de Educación, Cultura y Deporte (Spain).

Institutional Review Board Statement: Not applicable.

Informed Consent Statement: Not applicable.

Data Availability Statement: Primary data are available in Supplementary Tables S1–S4.

Conflicts of Interest: The authors declare no conflict of interest. The funders had no role in the design of the study; in the collection, analyses, or interpretation of data; in the writing of the manuscript; or in the decision to publish the results.

References

1. Cardone, L.; Castronuovo, D.; Perniola, M.; Cicco, N.; Candido, V. Saffron (*Crocus sativus* L.), the king of spices: An overview. *Sci. Hortic.* **2020**, *272*, 109560. [[CrossRef](#)]
2. Rubio Moraga, A.; Ahrazem, O.; Rambla, J.L.; Granell, A.; Gómez Gómez, L. Crocins with high levels of sugar conjugation contribute to the yellow colours of early-spring flowering crocus tepals. *PLoS ONE* **2013**, *8*, e71946. [[CrossRef](#)] [[PubMed](#)]
3. Frusciante, S.; Diretto, G.; Bruno, M.; Ferrante, P.; Pietrella, M.; Prado-Cabrero, A.; Rubio-Moraga, A.; Beyer, P.; Gomez-Gomez, L.; Al-Babili, S.; et al. Novel carotenoid cleavage dioxygenase catalyzes the first dedicated step in saffron crocin biosynthesis. *Proc. Natl. Acad. Sci. USA* **2014**, *111*, 12246–12251. [[CrossRef](#)]
4. Demurtas, O.C.; Frusciante, S.; Ferrante, P.; Diretto, G.; Azad, N.H.; Pietrella, M.; Aprea, G.; Taddei, A.R.; Romano, E.; Mi, J.; et al. Candidate Enzymes for Saffron Crocin Biosynthesis Are Localized in Multiple Cellular Compartments. *Plant Physiol.* **2018**, *177*, 990–1006. [[CrossRef](#)] [[PubMed](#)]
5. López-Jimenez, A.J.; Frusciante, S.; Niza, E.; Ahrazem, O.; Rubio-Moraga, Á.; Diretto, G.; Gómez-Gómez, L. A New Glycosyltransferase Enzyme from Family 91, UGT91P3, Is Responsible for the Final Glucosylation Step of Crocins in Saffron (*Crocus sativus* L.). *Int. J. Mol. Sci.* **2021**, *22*, 8815. [[CrossRef](#)] [[PubMed](#)]
6. Diretto, G.; Ahrazem, O.; Rubio-Moraga, Á.; Fiore, A.; Sevi, F.; Argandoña, J.; Gómez-Gómez, L. UGT709G1: A novel uridine diphosphate glycosyltransferase involved in the biosynthesis of picrocrocins, the precursor of safranal in saffron (*Crocus sativus*). *New Phytol.* **2019**, *224*, 725–740. [[CrossRef](#)]
7. Demurtas, O.C.; de Brito Francisco, R.; Diretto, G.; Ferrante, P.; Frusciante, S.; Pietrella, M.; Aprea, G.; Borghi, L.; Feeney, M.; Frigerio, L.; et al. ABC Transporters Mediate the Vacuolar Accumulation of Crocins in Saffron Stigmas. *Plant Cell* **2019**, *31*, 2789–2804. [[CrossRef](#)]
8. Xu, Z.; Pu, X.; Gao, R.; Demurtas, O.C.; Fleck, S.J.; Richter, M.; He, C.; Ji, A.; Sun, W.; Kong, J.; et al. Tandem gene duplications drive divergent evolution of caffeine and crocin biosynthetic pathways in plants. *BMC Biol.* **2020**, *18*, 63. [[CrossRef](#)]
9. Ahrazem, O.; Diretto, G.; Argandoña, J.; Rubio-Moraga, Á.; Julve, J.M.; Orzáez, D.; Granell, A.; Gómez-Gómez, L. Evolutionarily distinct carotenoid cleavage dioxygenases are responsible for crocetin production in *Buddleja davidii*. *J. Exp. Bot.* **2017**, *68*, 4663–4677. [[CrossRef](#)]
10. Diretto, G.; López-Jiménez, A.J.; Ahrazem, O.; Frusciante, S.; Song, J.; Rubio-Moraga, Á.; Gómez-Gómez, L. Identification and characterization of apocarotenoid modifiers and carotenogenic enzymes for biosynthesis of crocins in *Buddleja davidii* flowers. *J. Exp. Bot.* **2021**, *72*, 3200–3218. [[CrossRef](#)]
11. Frusciante, S.; Demurtas, O.C.; Sulli, M.; Mini, P.; Aprea, G.; Diretto, G.; Karcher, D.; Bock, R.; Giuliano, G. Heterologous expression of *Bixa orellana* cleavage dioxygenase 4-3 drives crocin but not bixin biosynthesis. *Plant Physiol.* **2022**, *188*, 1469–1482. [[CrossRef](#)] [[PubMed](#)]
12. Ahrazem, O.; Rubio-Moraga, A.; Berman, J.; Capell, T.; Christou, P.; Zhu, C.; Gómez-Gómez, L. The carotenoid cleavage dioxygenase CCD2 catalysing the synthesis of crocetin in spring crocuses and saffron is a plastidial enzyme. *New Phytol.* **2016**, *209*, 650–663. [[CrossRef](#)]
13. Zheng, X.; Mi, J.; Balakrishna, A.; Liew, K.X.; Ablazov, A.; Sougrat, R.; Al-Babili, S. Gardenia carotenoid cleavage dioxygenase 4a is an efficient tool for biotechnological production of crocins in green and non-green plant tissues. *Plant Biotechnol. J.* **2022**, *20*, 2202–2216. [[CrossRef](#)]

14. Martí, M.; Diretto, G.; Aragonés, V.; Frusciante, S.; Ahrazem, O.; Gómez-Gómez, L.; Daròs, J.A. Efficient production of saffron crocins and picrocrocin in *Nicotiana benthamiana* using a virus-driven system. *Metab. Eng.* **2020**, *61*, 238–250. [[CrossRef](#)] [[PubMed](#)]
15. Ahrazem, O.; Zhu, C.; Huang, X.; Rubio-Moraga, A.; Capell, T.; Christou, P.; Gómez-Gómez, L. Metabolic Engineering of Crocin Biosynthesis in *Nicotiana* Species. *Front. Plant Sci.* **2022**, *13*, 861140. [[CrossRef](#)] [[PubMed](#)]
16. Huang, X.; Morote, L.; Zhu, C.; Ahrazem, O.; Capell, T.; Christou, P.; Gómez-Gómez, L. The Biosynthesis of Non-Endogenous Apocarotenoids in Transgenic *Nicotiana glauca*. *Metabolites* **2022**, *12*, 575. [[CrossRef](#)]
17. Ahrazem, O.; Diretto, G.; Rambla, J.L.; Rubio-Moraga, A.; Lobato-Gómez, M.; Frusciante, S.; Argandoña, J.; Presa, S.; Granell, A.; Gómez-Gómez, L. Engineering high levels of saffron apocarotenoids in tomato. *Hortic. Res.* **2022**, *9*, uhac074. [[CrossRef](#)]
18. Bally, J.; Nakasugi, K.; Jia, F.; Jung, H.; Ho, S.Y.; Wong, M.; Paul, C.M.; Naim, F.; Wood, C.C.; Crowhurst, R.N.; et al. The extremophile *Nicotiana benthamiana* has traded viral defence for early vigour. *Nat. Plants* **2015**, *1*, 15165. [[CrossRef](#)]
19. Altschul, S.F.; Madden, T.L.; Schäffer, A.A.; Zhang, J.; Zhang, Z.; Miller, W.; Lipman, D.J. Gapped BLAST and PSI-BLAST: A new generation of protein database search programs. *Nucleic Acids Res.* **1997**, *25*, 3389–3402. [[CrossRef](#)]
20. Jefferson, R.A.; Kavanagh, T.A.; Bevan, M.W. GUS fusions: Beta-glucuronidase as a sensitive and versatile gene fusion marker in higher plants. *EMBO J.* **1987**, *6*, 3901–3907. [[CrossRef](#)]
21. Francisco, R.M.; Regalado, A.; Ageorges, A.; Burla, B.J.; Bassin, B.; Eisenach, C.; Zarrouk, O.; Vialet, S.; Marlin, T.; Chaves, M.M.; et al. ABCC1, an ATP binding cassette protein from grape berry, transports anthocyanidin 3-O-Glucosides. *Plant Cell* **2013**, *25*, 1840–1854. [[CrossRef](#)] [[PubMed](#)]
22. Bedoya, L.; Martínez, F.; Rubio, L.; Daròs, J.A. Simultaneous equimolar expression of multiple proteins in plants from a disarmed potyvirus vector. *J. Biotechnol.* **2010**, *150*, 268–275. [[CrossRef](#)] [[PubMed](#)]
23. Majer, E.; Navarro, J.A.; Daròs, J.A. A potyvirus vector efficiently targets recombinant proteins to chloroplasts, mitochondria and nuclei in plant cells when expressed at the amino terminus of the polyprotein. *Biotechnol. J.* **2015**, *10*, 1792–1802. [[CrossRef](#)] [[PubMed](#)]
24. Cordero, T.; Cerdán, L.; Carbonell, A.; Katsarou, K.; Kalantidis, K.; Daròs, J.A. Dicer-Like 4 Is Involved in Restricting the Systemic Movement of Zucchini yellow mosaic virus in *Nicotiana benthamiana*. *Mol. Plant-Microbe Interact. MPMI* **2017**, *30*, 63–71. [[CrossRef](#)]
25. Thole, V.; Worland, B.; Snape, J.W.; Vain, P. The pCLEAN dual binary vector system for *Agrobacterium*-mediated plant transformation. *Plant Physiol.* **2007**, *145*, 1211–1219. [[CrossRef](#)] [[PubMed](#)]
26. Larsen, E.; Christensen, L.P. Simple saponification method for the quantitative determination of carotenoids in green vegetables. *J. Agric. Food Chem.* **2005**, *53*, 6598–6602. [[CrossRef](#)]
27. Sulli, M.; Mandolino, G.; Sturaro, M.; Onofri, C.; Diretto, G.; Parisi, B.; Giuliano, G. Molecular and biochemical characterization of a potato collection with contrasting tuber carotenoid content. *PLoS ONE* **2017**, *12*, e0184143. [[CrossRef](#)]
28. Fraser, P.D.; Pinto, M.E.; Holloway, D.E.; Bramley, P.M. Technical advance: Application of high-performance liquid chromatography with photodiode array detection to the metabolic profiling of plant isoprenoids. *Plant J. Cell Mol. Biol.* **2000**, *24*, 551–558. [[CrossRef](#)]
29. Fantini, E.; Falcone, G.; Frusciante, S.; Giliberto, L.; Giuliano, G. Dissection of tomato lycopene biosynthesis through virus-induced gene silencing. *Plant Physiol.* **2013**, *163*, 986–998. [[CrossRef](#)]
30. Rodriguez-Amaya, D.B. *A Guide to Carotenoid Analysis in Foods*; ILSI Press: Washington, WA, USA, 1999.
31. Butnariu, M.; Rodino, S.; Petrache, P.; Negoescu, C.; Butu, M. Determination and quantification of maize zeaxanthin stability. *Dig. J. Nanomater. Biostructures* **2014**, *9*, 745–755.
32. Miller, N.J.; Sampson, J.; Candeias, L.P.; Bramley, P.M.; Rice-Evans, C.A. Antioxidant activities of carotenes and xanthophylls. *FEBS Lett.* **1996**, *384*, 240–242. [[CrossRef](#)] [[PubMed](#)]
33. Ordoudi, S.A.; Tsimidou, M.Z. Crocin bleaching assay (CBA) in structure-radical scavenging activity studies of selected phenolic compounds. *J. Agric. Food Chem.* **2006**, *54*, 9347–9356. [[CrossRef](#)]
34. Sarfarazi, M.; Jafari, S.M.; Rajabzadeh, G.; Feizi, J. Development of an environmentally-friendly solvent-free extraction of saffron bioactives using subcritical water. *LWT* **2019**, *114*, 108428. [[CrossRef](#)]
35. Franke, A.A.; Lai, J.F.; Halm, B.M. Absorption, distribution, metabolism, and excretion of isoflavonoids after soy intake. *Arch. Biochem. Biophys.* **2014**, *559*, 24–28. [[CrossRef](#)] [[PubMed](#)]
36. Hammer, Ø.; Harper, D.A.; Ryan, P.D. PAST: Paleontological statistics software package for education and data analysis. *Palaeontol. Electron.* **2001**, *4*, 9.
37. Ghag, S.B.; Adki, V.S.; Ganapathi, T.R.; Bapat, V.A. Plant Platforms for Efficient Heterologous Protein Production. *Biotechnol. Bioprocess Eng. BBE* **2021**, *26*, 546–567. [[CrossRef](#)]
38. Wei, X.; Su, X.; Cao, P.; Liu, X.; Chang, W.; Li, M.; Zhang, X.; Liu, Z. Structure of spinach photosystem II-LHCII supercomplex at 3.2 Å resolution. *Nature* **2016**, *534*, 69–74. [[CrossRef](#)]
39. Qin, X.; Suga, M.; Kuang, T.; Shen, J.R. Photosynthesis. Structural basis for energy transfer pathways in the plant PSI-LHCI supercomplex. *Science* **2015**, *348*, 989–995. [[CrossRef](#)]
40. Demurtas, O.C.; Nicolai, A.; Diretto, G. Terpenoid Transport in Plants: How Far from the Final Picture? *Plants* **2023**, *12*, 634. [[CrossRef](#)]

41. Gaillard, C.; Dufaud, A.; Tommasini, R.; Kreuz, K.; Amrhein, N.; Martinoia, E. A herbicide antidote (safener) induces the activity of both the herbicide detoxifying enzyme and of a vacuolar transporter for the detoxified herbicide. *FEBS Lett.* **1994**, *352*, 219–221. [[CrossRef](#)]
42. Molina-Hidalgo, F.J.; Vazquez-Vilar, M.; D'Andrea, L.; Demurtas, O.C.; Fraser, P.; Giuliano, G.; Bock, R.; Orzáez, D.; Goossens, A. Engineering Metabolism in Nicotiana Species: A Promising Future. *Trends Biotechnol.* **2021**, *39*, 901–913. [[CrossRef](#)] [[PubMed](#)]

Disclaimer/Publisher's Note: The statements, opinions and data contained in all publications are solely those of the individual author(s) and contributor(s) and not of MDPI and/or the editor(s). MDPI and/or the editor(s) disclaim responsibility for any injury to people or property resulting from any ideas, methods, instructions or products referred to in the content.